

Surface functionalized perovskite nanocrystals: Design strategy for organelle-specific fluorescence lifetime multiplexing

Anik Kumar Dey,^{a,f,†} Subhadeep Das,^{b,†} Sharon Mary Jose,^c Sreejesh Sreedharan,^d Noufal Kandoth,^e Surajit Barman,^c Abhijit Patra,^{b*} Amitava Das,^{e*} and Sumit Kumar Pramanik^{a,f*}

^aCSIR - Central Salt and Marine Chemicals Research Institute, Gijubhai Badheka Marg, Bhavnagar, Gujarat 364002; Email: sumitpramanik@csmcri.res.in

^bDepartment of Chemistry, Indian Institute of Science Education and Research Bhopal, India. E-mail: abhijit@iiserb.ac.in

^cDepartment of Biological Sciences, Indian Institute of Science Education and Research, Kolkata, Mohanpur, West Bengal, India.

^dHuman Science Research Centre, University of Derby, Kedleston road DE22 1GB, UK.

^eDepartment of Chemical Sciences and Centre for Advanced Functional Materials, Indian Institute of Science Education and Research, Kolkata, West Bengal, India. E-mail: amitava@iiserkol.ac.in

^fAcademy of Scientific and Innovative Research (AcSIR), CSIR-Human Resource Development Centre, Ghaziabad, Uttar Pradesh 201 002, India

† Equal contribution

S. No.	Content	Page
1	Materials	S2
2	Methodologies [Synthesis, cell culture, intracellular imaging, MTT assay, fluorescence lifetime multiplexing]	S2-S7
3	Characterization data for SiO ₂ @Pv-NCs [FTIR, EDX (TEM), ξ potential plot]	S8-S9
4	Characterization data for [SiO ₂ @Pv-NCs]tpm and [SiO ₂ @Pv-NCs]tsy [TEM, EDX, DLS, XPS, ξ potential plot, steady-state luminescence spectra and excited state luminescence decay studies]	S10-S14
5	Stability of functionalized Pv-NCs in blood serum	S14
6	MTT assay details and stability of SiO ₂ @Pv-NCs in blood serum	S15
7	Confocal images/results of the temperature-dependent cellular uptake studies/results on the probe stability as an imaging reagent	S16-S18
8	Intracellular photostability, organelle dynamics, long-term imaging, and fluorescence lifetime multiplexing data	S19-S22
9	References	S23

Materials

Cesium carbonate (Cs_2CO_3), lead bromide (PbBr_2), oleic acid (OA), oleylamine (OLA), octadecene (ODE), (3-mercaptopropyl)trimethoxy silane, triphenylphosphine (PPh_3), allyl Bromide, allyl amine and *p*-toluene sulfonyl chloride were purchased from TCI, Japan. Toluene and DCM were purchased from Merck, India. Dulbecco's modified Eagle medium (DMEM), phosphate-buffered saline (PBS, 1X), trypsin-EDTA solution (0.25%), fetal bovine serum (FBS), penicillin-streptomycin-glutamine (PSG 100X), formaldehyde (Sigma-Aldrich, F8775-25ML, methanol content ~10-15%), ERTracker™ Red, MitoTracker™ Deep Red, [3-(4,5-dimethylthiazol-2-yl)-2,5-diphenyltetrazolium bromide (MTT), and FluoroBrite™ DMEM were collected from ThermoFisher Scientific. Formaldehyde (~10% methanol, F8775-25ML) was obtained from Sigma-Aldrich.

Synthesis Method

Preparation of Cs-oleate:

The synthesis was conducted under inert conditions using a Schlenk line setup following a reported procedure.¹ Cs_2CO_3 (267 mg, 0.82 mM) and oleic acid (0.833 mL, 2.56 mM) were mixed in a 3-neck flask with 10 mL ODE. The mixture was then degassed under nitrogen flow and heated at 130 °C for 10 min. The temperature was gradually raised to 150 °C and heated for 10 min until the solution became transparent. This was then brought to room temperature and used as such for further reaction.

Synthesis of Pristine CsPbBr_3 Quantum Dots (Pv-NCs):

This was prepared following a reported procedure with a few modifications.² PbBr_2 (138 mg, 0.38 mM), OA (1 mL, 3 mM), and 1 mL OLA were mixed in a 3-neck flask with 10 mL ODE. This mixture was degassed under nitrogen flow and heated at 130 °C for 1 hr. Then, the temperature was gradually raised to 180 °C for 10 min with stirring. After that freshly prepared Cs-oleate (1 mL) was injected quickly into the mixture with constant stirring in an ice bath for 30 sec to yield green emissive quantum dots. The product (Pv-NCs) was collected via centrifugation at 11,000 rpm and dispersed in 4 mL toluene.

Synthesis of silica-coated CsPbBr_3 quantum dots (SiO_2 @Pv-NCs):

A reported procedure was adopted for the preparation of these silica-coated Pv nanocrystals (SiO_2 @Pv-NCs) with necessary modifications.² A homogenized dispersion of Pv-NCs (2 mL) in toluene was taken, and 5 μL 3-mercaptopropyltrimethoxy silane was added. The whole solution was stirred for 1 hr. Following this, a solution of 15 mL toluene containing 25 μL 3-mercaptopropyltrimethoxysilane and 2 μL Milli-Q water was added. The whole reaction mixture was placed for heating at 45 °C for 36 h in an RB flask fitted with a condenser, open to the air. Then, the reaction mixture was cooled to room temperature, and SiO_2 @Pv-NCs were collected via centrifugation.

Synthesis of Ligand PHOS-1:

PHOS-1 was synthesized following a reported procedure.³ Triphenylphosphine (300 mg, 1.144 mmol) and allyl bromide (0.2 mL, 2 mmol) were taken in 20 mL of toluene. The whole solution was refluxed overnight under constant stirring, and a white precipitate was obtained. This white precipitate was filtered out and washed out with toluene. Isolated solid (yield: 81%) had the desired purity for further use. ¹H NMR (500 MHz, d₆-DMSO, δ): 7.37 (m, 15H), 5.34 (m, 2H), 4.58 (dd, *J* = 6 Hz, 8 Hz, 2H), 2.13 (d, *J* = 5 Hz, 1H); ¹³C NMR (125 MHz, d₆-DMSO, δ): 162.7, 138.4, 137.1, 133.6, 121.2, 30.0, 24.9; ESI Ms Analysis: *m/z* (Calc.) 303.25 and (Expt.) 303.1532.

Synthesis of Ligand ER-1:

ER-1 was synthesized following a reported procedure.³ *p*-Toluenesulfonylchloride (419.63 mg, 2.2 mmol) and allyl amine (187.3 mg, 2 mmol) were taken in 10 mL dry DCM and stirred for 24 h at room temperature. Then 1(M) HCl was added, and the desired product was extracted in the DCM layer through solvent extraction. This DCM solution was kept with anhydrous sodium sulphate for about an hour, and then the whole solution was dried under reduced pressure to yield (76%) the desired product in a pure state. ¹H NMR (500 MHz, d₆-DMSO, δ): 7.74 (d, *J* = 6.5 Hz, 2H), 7.30 (d, *J* = 6.5 Hz, 2H), 5.71 (m, 1H), 5.15 (d, *J* = 14.5 Hz, 1H), 5.08 (d, *J* = 8.5 Hz, 1H), 4.52 (s, 1H), 3.57 (d, *J* = 4.5 Hz, 2H), 2.42 (s, 1H); ¹³C NMR (500 MHz, d₆-DMSO, δ): 143.6, 137.0, 133.1, 129.8, 127.2, 117.9, 46.0, 21.6; ESI Ms: *m/z* (Calc.) 212.0364 and (Expt.) 212.0350.

Surface modification of SiO₂@Pv-NCs with PHOS-1 for generation of [SiO₂@Pv-NCs]tpm:

10 mg PHOS-1 was added to a 5 mL solution of SiO₂@Pv-NCs (10 mg) and was irradiated with UV light for 30 seconds. An OMNICURE Series 1000 lamp system with a four-arm setting was used as a UV light source for irradiation. The system was equipped with a 100 W high-pressure mercury vapour short arc lamp. Using an iris setting of 50%, the sample was irradiated for 30 sec. Then, the product was collected via centrifugation.

Surface modification of SiO₂@Pv-NCs with ER-1 for generation of [SiO₂@Pv-NCs]tsy:

10 mg ER-1 was added to a 5 mL solution of silica-coated quantum dots (10 mg) and placed in UV light for 30 seconds. An OMNICURE Series 1000 lamp system with a four-arm setting was used as a UV light source for irradiation. The system was equipped with a 100 W high-pressure mercury vapour short arc lamp. Using an iris setting of 50%, the sample was irradiated for 30 sec. While one of the UV lamp arms illuminated the sample from the top, the other three arms were used for illumination from different sides of the vial. Then, the product was collected via centrifugation.

The luminescent property of the Pv-NCs and surface functionalized nanocrystals is highly dependent upon the size of the perovskite core as well as the thickness of the silica shell.⁴

Instrumentation and Experimental Procedures:

^1H NMR and ^{13}C NMR were recorded using a Bruker AX 500 spectrometer (500 MHz) at 25°C. TMS was used as an internal reference during NMR spectroscopic study. Parkin Elmer 883 spectrometer was used to record the FT-IR data using the KBr pellet. UV-Vis absorption spectra were recorded using a Shimadzu UV-2600 spectrophotometer. Fluorescence spectra were recorded at room temperature using a PTI QuantaMaster 400 spectrofluorometer. Using a Zetasizer Nano-ZS90 (Malvern) instrument with a 632.8 nm He-Ne laser DLS, experiments were carried out at 298 K. Transmission electron microscopy images were collected using a JEOL JEM-2100 electron microscope working at 200 kV accelerating voltage. The samples were prepared on the surface of lacey-carbon-supported copper TEM grids. Using a Q-of-micro quadrupole mass spectrophotometer (Micromass), ESI-MS was done. Powder X-ray diffraction (PXRD) patterns were recorded at room temperature on a Philips X'pert X-ray powder diffractometer using Cu-K α radiation ($\lambda = 1.5418 \text{ \AA}$) in the 2θ range of 5-50°. XPS analysis was carried out using a Thermo Scientific ESCALAB 250 Xi photoelectron spectrometer (XPS) using a monochromatic Al K α X-ray as an excitation source. Edinburgh instrument OB 920 spectrofluorometer was used for performing lifetime experiments (TCSPC).

Cell culture: HeLa cells were obtained from the National Centre for Cell Science (NCCS) Pune, India. In tissue culture dishes (Tarsons, 60 mm), HeLa cells were cultured with phenol red containing DMEM, supplemented with 1% (v/v) PSG and 10% (v/v) FBS under humid conditions, *i.e.*, 5% CO₂, 37 °C. The grown cells were trypsinized and transferred to confocal dishes (SPL life sciences, 35 mm) before 24 h of imaging. The grown cells in confocal dishes were then washed thrice with PBS, and the nanocrystal or commercial tracker dye containing DMEM (2 mL) was added to the confocal dishes. The cells were incubated with the nanocrystals ($5 \times 10^{-4} \text{ g mL}^{-1}$) for 30 mins if not otherwise specified. The commercial tracker dyes (0.5 μM) were incubated for 10 mins in humid conditions before imaging. After the probe incubation, PBS was used to wash the cells thrice, and FluoroBrite™ DMEM (2 mL) was added before imaging.

To check the long-term imaging ability of the nanocrystals, HeLa cells were first grown in 35 mm confocal dishes (cell density ~ 1000 cells per well) and incubated with the probe ($5 \times 10^{-4} \text{ g mL}^{-1}$) for 30 mins under 37 °C and 5% CO₂ environment. The excess dye was removed by washing the cells thrice with PBS, fresh DMEM (2 mL) was added, and the cells were incubated for 1 - 3 days separately. On each day, previous media was discarded, cells were washed with PBS (once), and fresh growth media (2 mL) was added to maintain healthy conditions for cell growth. On respective days after incubation, the cells were washed with PBS, and FluoroBrite™ DMEM solution (2 mL) was added before imaging.

FLIM studies (Procedure): For fluorescence multiplexing studies, HeLa cells were grown in a 10 mm confocal and coincubated with [SiO₂@Pv-NCs]t_{sy} ($2 \times 10^{-4} \text{ mg mL}^{-1}$) and [SiO₂@Pv-NCs]t_{pm} ($2 \times 10^{-4} \text{ mg mL}^{-1}$) in DMEM (2 mL) for 20 mins each. The cells were then washed with PBS thrice, and FluoroBrite™ DMEM solution (2 mL) was added before imaging.

Fluorescence microscopy: PicoQuant, MicroTime 200 clubbed with Olympus IX-73 (inverted optical microscope, 60x lens, water objective, numerical aperture 1.20) was used for intracellular photostability, fluorescence imaging, long-term imaging, fluorescence lifetime imaging microscopy (FLIM) and fluorescence lifetime multiplexing of biological samples using the time-tagged time-resolved (TTTR) mode.⁵ Time-correlated single photon counting (TCSPC) studies were performed to evaluate the average fluorescence decay time constants for [SiO₂@Pv-NCs]tpm and [SiO₂@Pv-NCs]tsy using Delta Flex-01-DD (HORIBA) spectrometer ($\lambda_{\text{ex}} = 470$ nm). For TCSPC studies, instrument response functions (IRF) were recorded to understand the minimum measurable lifetime for the excitation source used for individual experiments. For cellular imaging of only nanocrystals incubated samples, 470 nm laser excitation (repetition rate = 20 MHz) was used. A suitable long-pass filter (488 nm) was used to collect the sample's fluorescence, avoiding any excitation signal. For colocalization and photostability studies, the nanocrystals were excited at 470 nm, and fluorescence was collected within the wavelength range of 500 - 540 nm, and the commercial dyes were excited at 640 nm, and fluorescence was collected within the wavelength range of 650 - 690 nm. To compare the photostability of the organelle targeting nanocrystals with commercial tracker dyes, the co-incubated cells were irradiated under constant laser power (0.3 μ W). The laser power density was calculated using the following equation.

$$\text{Power density} = \frac{\text{Laser power}}{\pi r^2}$$

Where, r = radius of the laser beam = 0.25 μ m.

The laser power density was found to be 1.52 W mm⁻².

The images for fluorescence multiplexing studies were recorded using a 470 nm (repetition rate = 20 MHz) laser. A suitable long-pass filter (488 nm) was used to collect the fluorescence signals from the sample, avoiding any excitation signal.

Cellular Uptake and confocal imaging of [SiO₂@Pv-NCs]tpm and [SiO₂@Pv-NCs]tsy:

To check the cellular uptake of the nanocrystals, grown HeLa cells plated in confocal dishes were first incubated at different temperatures (4 °C, 20 °C, and 37 °C) in complete growth media for 1 h. Then, the cells were treated with the respective nanocrystals ([SiO₂@Pv-NCs]tpm and [SiO₂@Pv-NCs]tsy) for 30 min under a 5% CO₂ environment. The cells were washed with PBS (2 mL) thrice, and FluoroBrite™ DMEM (2 mL) was added to the cells before imaging using a confocal microscope.

For fixed cell imaging, the HeLa cells were grown on coverslips (22 mm × 22 mm, 170 ± 5 μ m square cover glasses) placed in six-well plates in Dulbecco's Modified Eagle's medium (containing 10% FBS and 1% penicillin-streptomycin) for 24 h at 37 °C under 5% CO₂ gas. The confluent cells were then washed with PBS thrice. The cells were fixed in 4% formaldehyde (2 mL PBS) for 5 min. The fixed cells were washed thrice with PBS and were stained with the nanocrystal dispersion in PBS (30 min incubation). After the incubation, the cells were washed with PBS

thrice, and slides were used for confocal imaging. Commercial formaldehyde solutions contain ~10% methanol, which is a known permeabilizing agent. This allows the localization of the synthesized nanocrystals into the cell. In the present study, we have used commercial formaldehyde (Sigma-Aldrich, F8775-25ML, methanol content ~10-15%) to prepare a 4% formaldehyde solution in PBS, and then the cells were fixed.⁶ The fixation process itself allowed the successful intracellular localization of the nanocrystals.

Strong physisorption of the amine/thiol functionalities of the mitochondrial proteins on silica surfaces is also expected to favour the retention of the ([SiO₂@Pv-NCs]tpm and allows the dye to maintain its intramitochondrial localization even after a loss in mitochondrial membrane potential.^{6b}

Further, fixation with paraformaldehyde (PFA) can inhibit cell autolysis, retain cell components, maintain cell morphology and structural integrity, and make the microscopic appearance of cells more apparent. Mitochondria are highly dynamic organelles. Thus, the effective cross-link ability of PFA is beneficial for preserving their antigenicity and morphology.⁷

MTT assay:

HeLa cells were seeded at 6000 cells per well in a 96-well flat bottom plate together with 200 μ L of Dulbecco's Modified Eagle's medium culture, supplemented with 1 % penicillin-streptomycin and 10 % Fetal Bovine Serum. The cells were left to incubate at 37 °C in a 5 % CO₂ incubator for 24 h after which cells were washed with 1X PBS. A total of six wells per condition were taken, and 200 μ L of the different required conditions were added to the respective wells: blank (supplemented Dulbecco's Modified Eagle's Medium), cells with the same medium (basal), 5 x 10⁻⁴ mg mL⁻¹ of [SiO₂@Pv-NCs]tpm or [SiO₂@Pv-NCs]tsy in supplemented Dulbecco's Modified Eagle's Medium (test). The cells were left to incubate for 24, 48, or 72 hrs in the incubator, after which they were washed once with 1X PBS. Then 200 μ L of MTT solution (0.2 mg mL⁻¹ in PBS) in supplemented Dulbecco's Medium was added to each well and left to incubate for an additional 4 hours to allow the formazan complex to form. Then, this solution was aspirated, and 200 μ L DMSO was added into the wells, and the absorbance was measured at 570 nm. The data are represented as the average cell viability obtained by this formula: (average test OD/average control OD) \times 100 (n = 6).

Fluorescence lifetime multiplexing:

The fluorescence decay profiles of the organelle-specific nanocrystals were best fitted with a bi-exponential model (Fig. S10). Since the probes have two decay components and close lifetime values, the probability of observing overlapping decay components at a spot where mitochondria and ER are both present cannot be overruled. In these circumstances, deconvolution based on lifetime fitting could be challenging and often inconclusive.⁸ Thus, rather than fitting the decay profile and deconvoluting each lifetime component and contributions from the cells co-incubated with [SiO₂@Pv-NCs]tpm and [SiO₂@Pv-NCs]tsy, we have performed pattern matching analysis

for the fluorescence lifetime multiplexing studies, using the pre-obtained lifetime decays of cells individually incubated with [SiO₂@Pv-NCs]tpm and [SiO₂@Pv-NCs]tsy.

For fluorescence lifetime multiplexing, first, the intracellular decay profiles and fluorescence lifetime imaging microscopy (FLIM) images of HeLa cells singly incubated with [SiO₂@Pv-NCs]tpm and [SiO₂@Pv-NCs]tsy were recorded. These decay profiles were later used as a reference for fitting the FLIM image of [SiO₂@Pv-NCs]tpm and [SiO₂@Pv-NCs]tsy co-incubated samples. Then, the FLIM images of HeLa cells co-incubated with [SiO₂@Pv-NCs]tpm and [SiO₂@Pv-NCs]tsy were recorded. The composite decay profile obtained from the FLIM image of the dual-incubated sample was then fitted by performing the pattern matching analysis using the previously recorded intracellular decays.⁸ After the analysis, the residuals of the initial fit were checked before the deconvolution of the FLIM image. According to the reference decay profiles, the probes that most likely belong with an average decay time of $\tau_{\text{avg}} \sim 2.1$ ns and $\tau_{\text{avg}} \sim 3.1$ ns were deconvoluted.

Further analysis using advanced algorithms, comparing error levels from various methods, or conducting frequency domain multiplexing analysis could further strengthen the scope of fluorescence probes exhibiting multi-exponential decays for lifetime multiplexing.^{8,9}

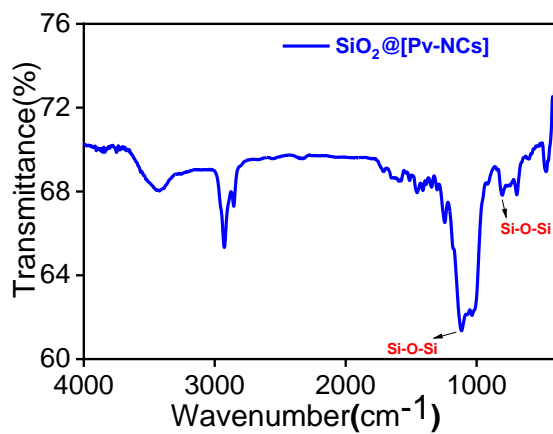


Fig. S1. FT-IR Spectrum of SiO₂@Pv-NCs (as KBr pellet).

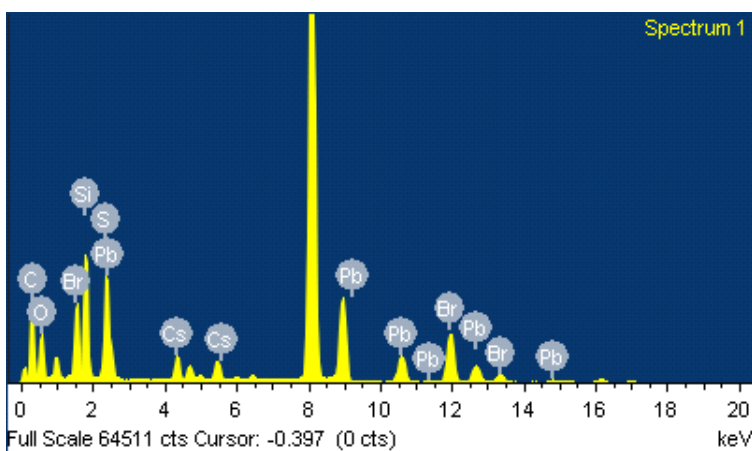


Fig. S2. The EDX result of SiO₂@Pv-NCs. The presence of the elements Si, S, and O clearly shows the successful encapsulation of the Pv-NCs as the core and the silica-based (SiO₂) surface as the shell.

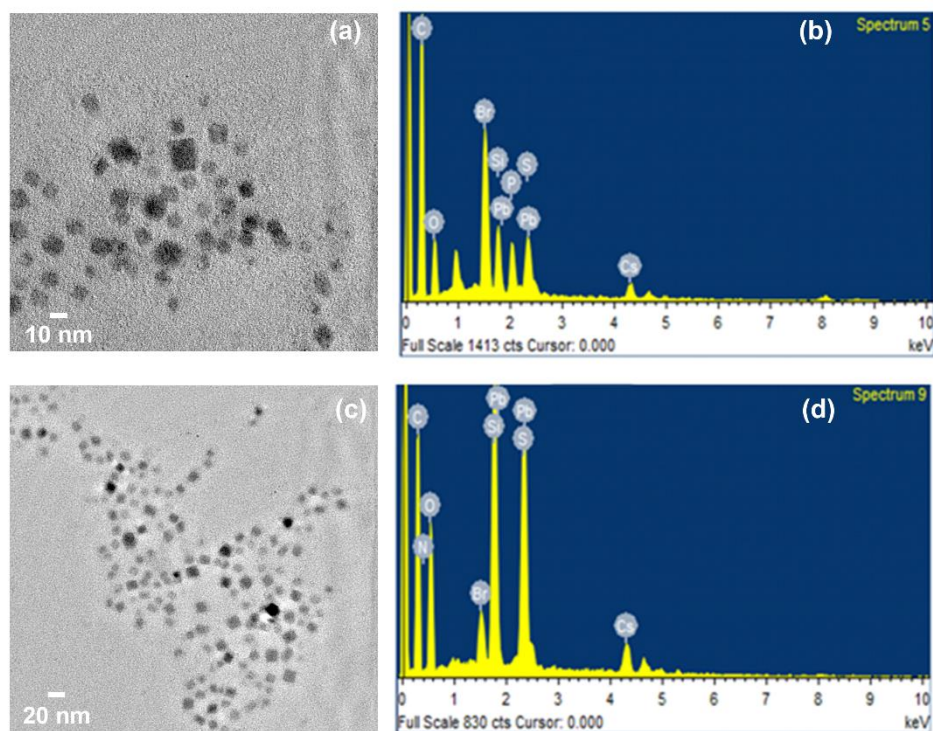


Fig. S3. (a) TEM images of $[\text{SiO}_2@\text{Pv-NCs}]_{\text{tpm}}$; scale = 10 nm. (b) The EDX result of $[\text{SiO}_2@\text{Pv-NCs}]_{\text{tpm}}$. The presence of elements P and C clearly shows the successful post-grafting of triphenylphosphine functionalities on the surface as the shell. (c) TEM images of $[\text{SiO}_2@\text{Pv-NCs}]_{\text{tsy}}$; scale = 20 nm. (d) The EDX profile of $[\text{SiO}_2@\text{Pv-NCs}]_{\text{tsy}}$. The presence of the elements S and N clearly shows the successful post-grafting of tosyl functionalities on the surface as the shell.

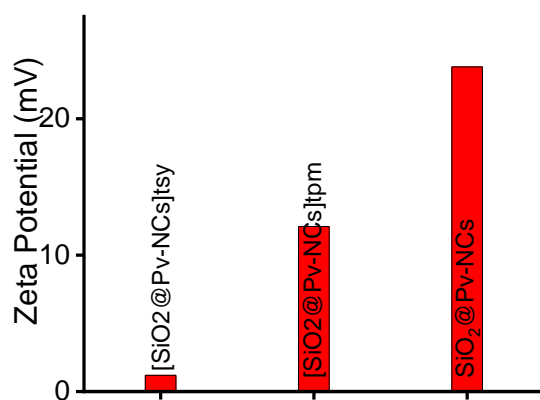


Fig. S4. Zeta potential plot of $\text{SiO}_2@[\text{Pv-NCs}]_{\text{tsy}}$, $\text{SiO}_2@[\text{Pv-NCs}]_{\text{tpm}}$, and $\text{SiO}_2@[\text{Pv-NCs}]$.

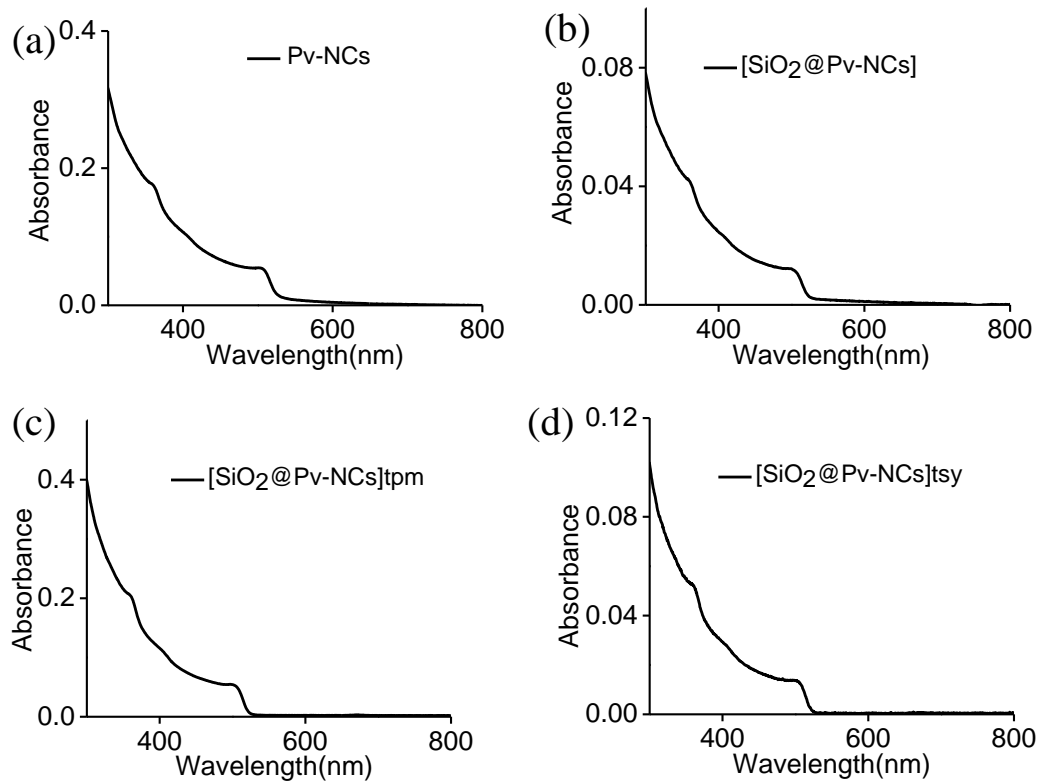


Fig. S5. Absorption spectra of (a) Pv-NCs, (b) SiO₂@Pv-NCs, (c) [SiO₂@Pv-NCs]tpm, and (d) [SiO₂@Pv-NCs]tsy.

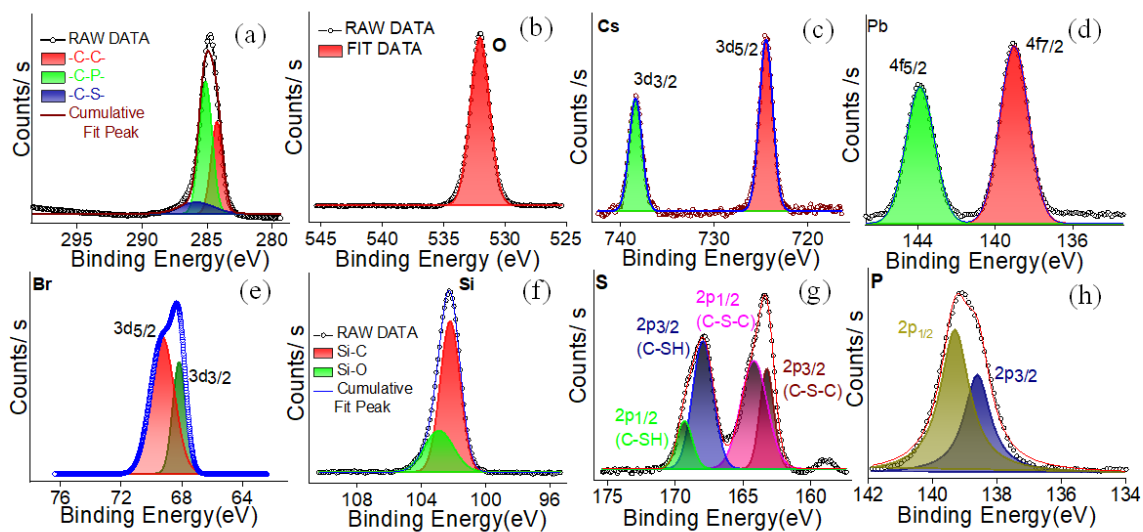


Fig. S6. (a-h) High-resolution XPS Spectra of C (1s), O (1s), Cs (3d), Pb (4f), Br (3d), Si (2p), S (2p), and P (2p), respectively of SiO₂@[Pv-NCs]tpm.

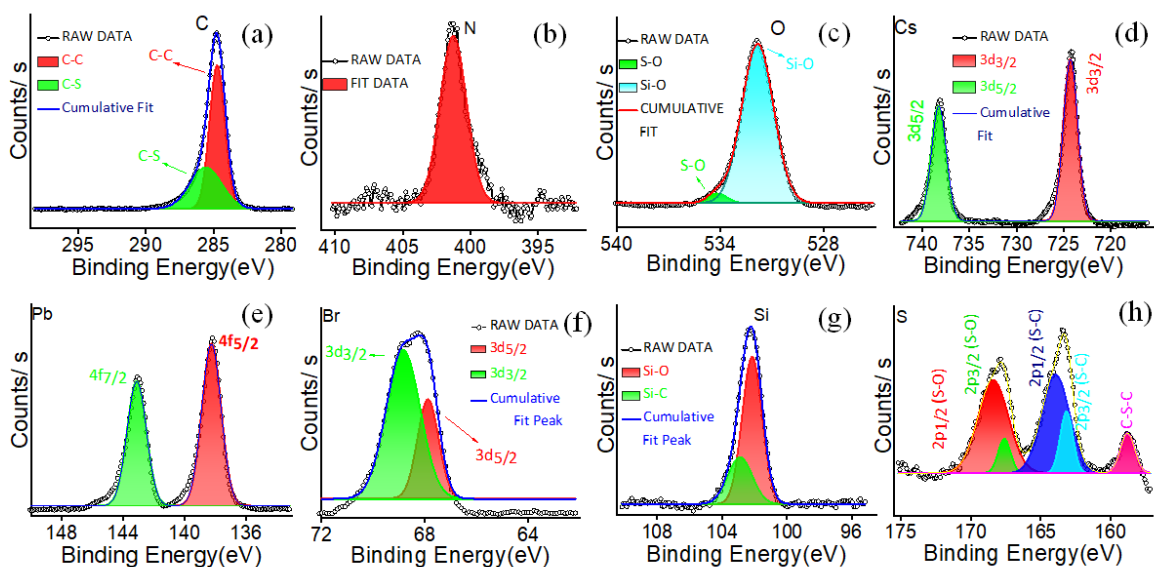


Fig. S7. (a-h) High-resolution XPS Spectra of C (1s), N (1s), O (1s), Cs (3d), Pb (4f), Br (3d), Si (2p), and S (2p), respectively of SiO₂@[Pv-NCs]tsty.

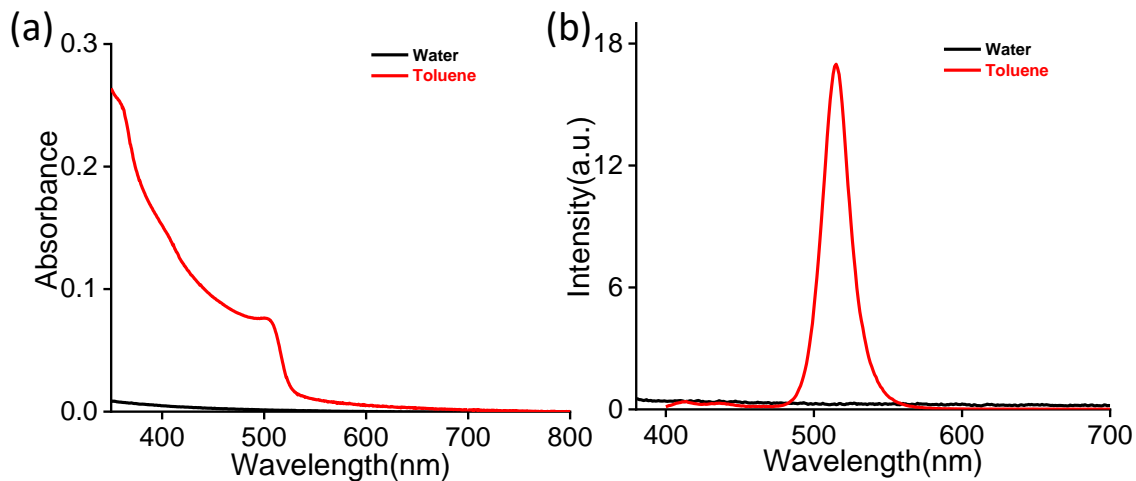


Fig. S8. (a) Absorption spectra of Pv-NCs in water and toluene. (b) Emission spectra of Pv-NCs in water and toluene.

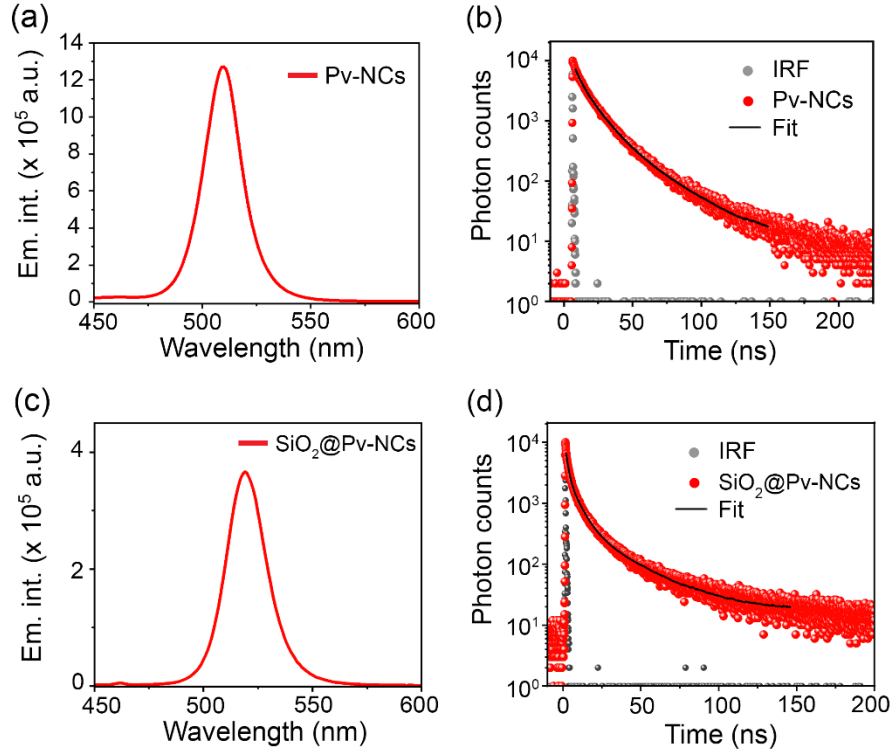


Fig. S9. (a) Emission spectra of Pv-NCs in toluene. (b) Photoluminescence decay profile of Pv-NCs in toluene, suggesting multi-exponential decay with an average lifetime, $\tau_{\text{avg}} = 15.2$ ns ($\lambda_{\text{ex}} = 470$ nm, $\lambda_{\text{em}} = 515$ nm). (c) Emission spectra of SiO₂@Pv-NCs in water. (d) Photoluminescence decay profile of SiO₂@Pv-NCs in water, suggesting multi-exponential decay with an average lifetime, $\tau_{\text{avg}} = 14.3$ ns ($\lambda_{\text{ex}} = 470$ nm, $\lambda_{\text{em}} = 520$ nm). The instrument response function (IRF) is depicted in grey in (b) and (d).

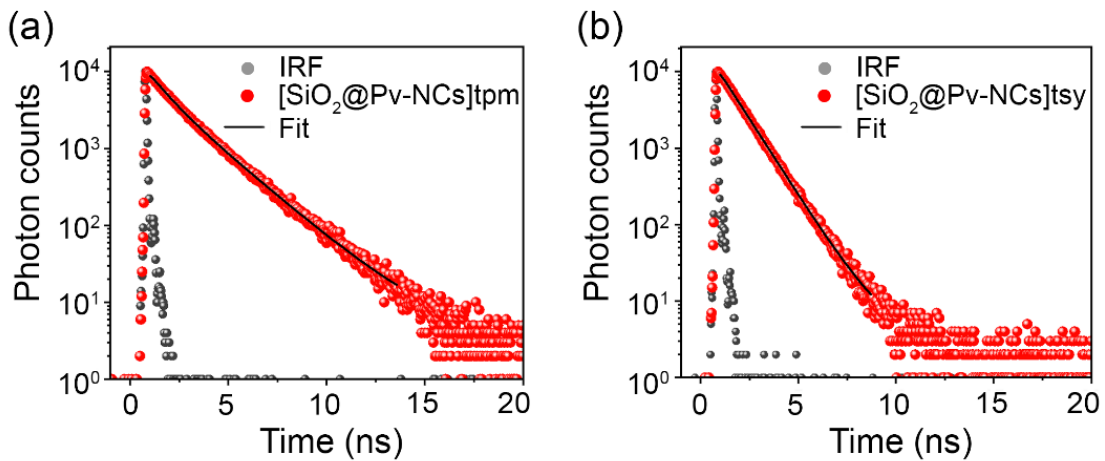


Fig. S10. (a) Time-resolved decay of [SiO₂@Pv-NCs]tpm in water; $\tau_1 = 1.7$ ns (27%), $\tau_2 = 3.8$ ns (73%), $\tau_{\text{avg}} = 3.2$ ns, ($\lambda_{\text{ex}} = 470$ nm, $\lambda_{\text{em}} = 520$ nm). (b) Time-resolved decay of [SiO₂@Pv-NCs]tsy in water; $\tau_1 = 1.1$ ns (2.6%), $\tau_2 = 2.2$ ns (97.4%), $\tau_{\text{avg}} = 2.2$ ns, ($\lambda_{\text{ex}} = 470$ nm, $\lambda_{\text{em}} = 520$ nm). The instrument response function (IRF) is depicted in grey in (a) and (b).

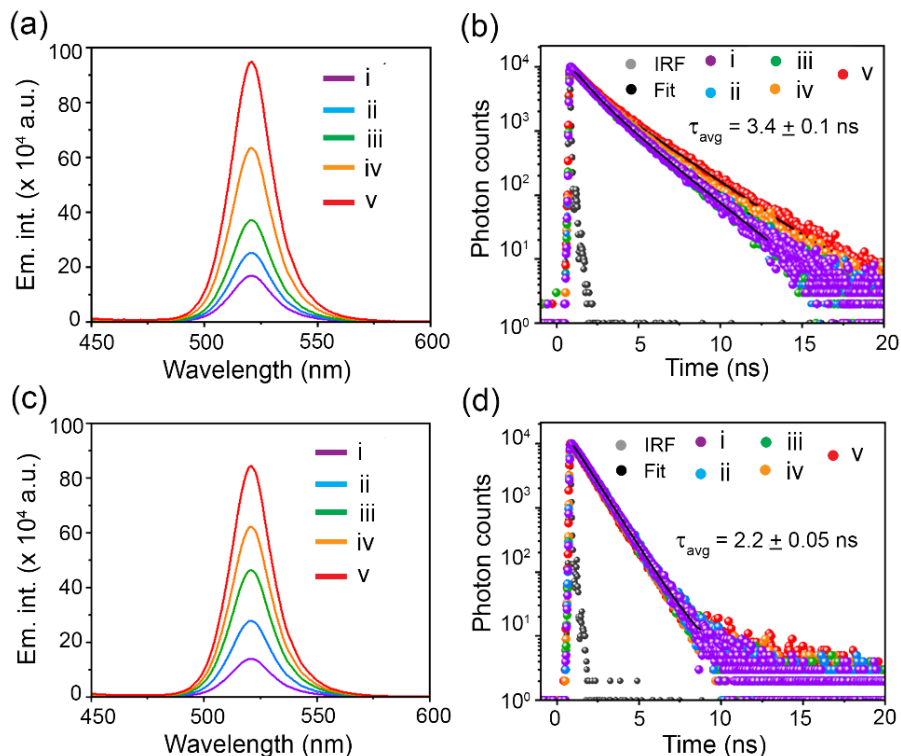


Fig. S11. (a) Emission and (b) decay profiles of $[\text{SiO}_2@\text{Pv-NCs}]_{\text{tpm}}$ at different concentrations ($\lambda_{\text{ex}} = 470 \text{ nm}$, $\lambda_{\text{em}} = 525 \text{ nm}$). (c) Emission and (d) decay profiles of $[\text{SiO}_2@\text{Pv-NCs}]_{\text{tsy}}$ at different concentrations ($\lambda_{\text{ex}} = 470 \text{ nm}$, $\lambda_{\text{em}} = 520 \text{ nm}$). The legends indicate (i) 1.5, (ii) 2, (iii) 5, (iv) 8, and (v) $10 \times 10^{-4} \text{ mg mL}^{-1}$ of the nanocrystals in milli-Q water.

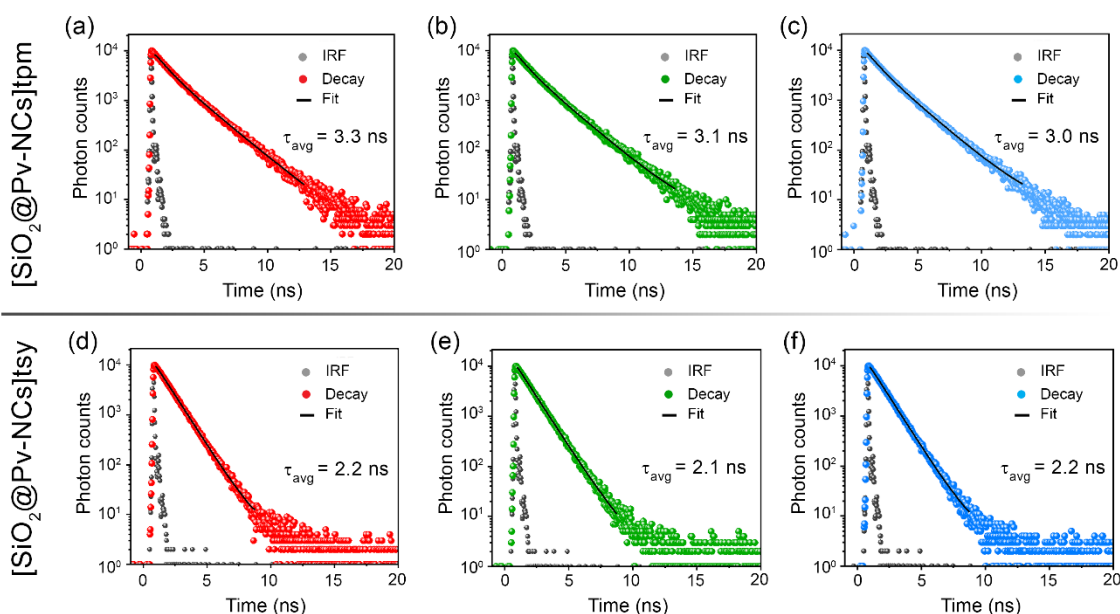


Fig. S12. Fluorescence decay profiles of (a-c) $[\text{SiO}_2@\text{Pv-NCs}]_{\text{tpm}}$ and (d-f) $[\text{SiO}_2@\text{Pv-NCs}]_{\text{tsy}}$; conc: $5 \times 10^{-4} \text{ mg mL}^{-1}$, $\lambda_{\text{ex}} = 470 \text{ nm}$, $\lambda_{\text{em}} = 520 \text{ nm}$ in milli-Q water.

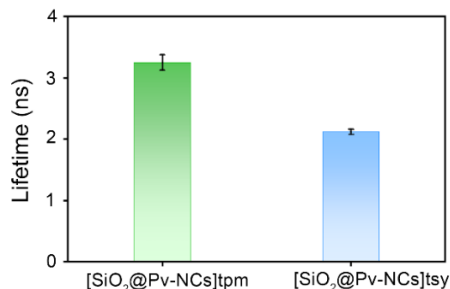


Fig. S13. Bar diagrams depicting the variation of average fluorescence lifetimes of [SiO₂@Pv-NCs]tpm and [SiO₂@Pv-NCs]tsy; the error bars are plotted based on triplicate measurements (conc: 5×10^{-4} mg mL⁻¹, $\lambda_{\text{ex}} = 470$ nm, $\lambda_{\text{em}} = 520$ nm).

Stability of [SiO₂@Pv-NCs]tpm and [SiO₂@Pv-NCs]tsy in serum solution

A male Wistar rat was used to collect 3 mL of blood by piercing the retro-orbital plexus using an EDTA-coated vacutainer. After the obtained blood was centrifuged at 1000 rpm for 15 minutes. Following this, blood serum was collected for our experiments. These stability experiments were performed at the research laboratory of Prof. Surajit Ghosh of the Department of Bioscience & Bioengineering, IIT Jodhpur (India). The dispersion stability of the [SiO₂@Pv-NCs]tpm and [SiO₂@Pv-NCs]tsy and their serum-induced aggregation were evaluated spectrophotometrically by UV-visible spectrophotometer at 25 °C (Fig. S14). The normalized integrated absorbance (NIA) between 600 and 750 nm was used as an indicator of aggregate formation. The NIA is defined as follows:

$$NIA(t) = (A_t - A)/A$$

where A is the initial integrated absorbance between 600 and 750 nm, and A_t is the integrated absorbance between 600 and 750 nm, t hours after the addition of 100 % blood serum.

It can be seen that after their incubation in 100 % serum for 30 h, the integrated absorbance values for both [SiO₂@Pv-NCs]tpm and [SiO₂@Pv-NCs]tsy remained unchanged (Fig. S14b). This indicates both [SiO₂@Pv-NCs]tpm and [SiO₂@Pv-NCs]tsy are highly stable under physiological conditions.

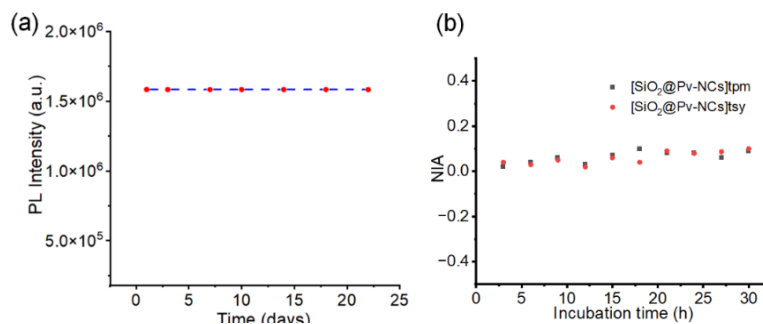


Fig. S14. (a) Water stability tests of SiO₂@Pv-NCs in distilled water; PL intensity is recorded at regular intervals of time ($\lambda_{\text{em}} = 525$ nm). The SiO₂@Pv-NCs retain about 99.5 % of their initial PL intensity even after 22 days. (b) Normalized integrated absorbance (NIA) vs time (h) plot. NIA between 600 and 750 nm was used as an indicator of aggregate formation and is evaluated spectrophotometrically by UV-visible spectrophotometer at 25 °C.

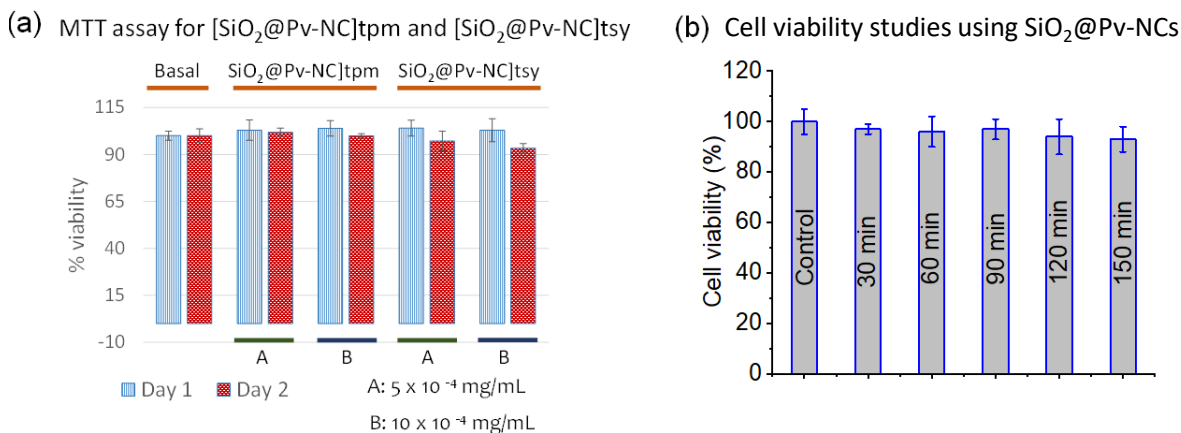


Fig. S15. (a) MTT assay for [SiO₂@Pv-NCs]tpm and [SiO₂@Pv-NCs]tsy with live HeLa cells after incubation for 24 or 48 h following standard protocol. (b) Cell viability of HeLa cells with exposure to 400 nm light with 100 µg/mL of SiO₂@Pv-NCs for up to 150 min, determined using the MTT assay. For the control sample, no light was given. Data represent the mean ± standard deviation of three replicates.

MTT assay suggests that cell viability levels remained stable as compared to a control group; no decrease below 94 % was observed after exposure (24, 48 h) to different concentrations (5×10^{-4} mg/mL and 10×10^{-4} mg/mL) of [SiO₂@Pv-NCs]tpm and [SiO₂@Pv-NCs]tsy. This confirms that the synthesized hybrid Pv-NCs are biocompatible (Fig. S15a). One of the concentrations used is notably higher than the range used for CLSM imaging studies.

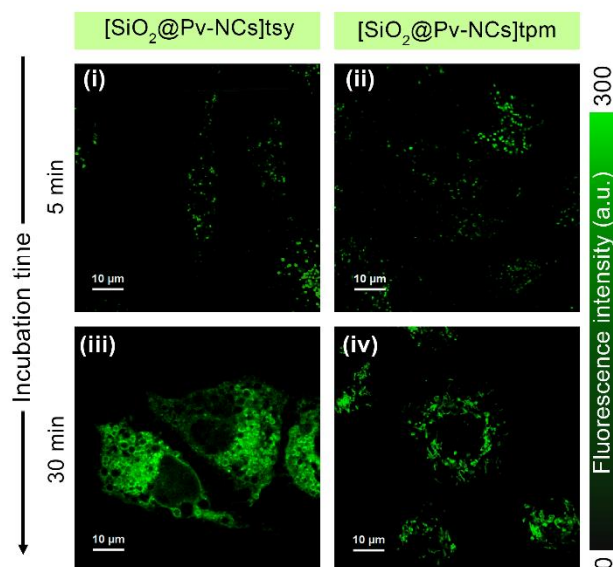


Fig. S16. Confocal laser scanning microscopy (CLSM) images of live HeLa cells treated with (i, iii) [SiO₂@Pv-NCs]tsy, and (ii, iv) [SiO₂@Pv-NCs]tpm; HeLa cells were incubated with the nanocrystals for (i, ii) 5 mins and (iii, iv) 30 mins; $\lambda_{ex} = 470$ nm, $\lambda_{em} = 488 - 800$ nm, scale = 10 µm. The images indicate punctate-like trapped nanocrystals in endosomes at the early stages of incubation (5 mins). A common intensity scale is also presented.

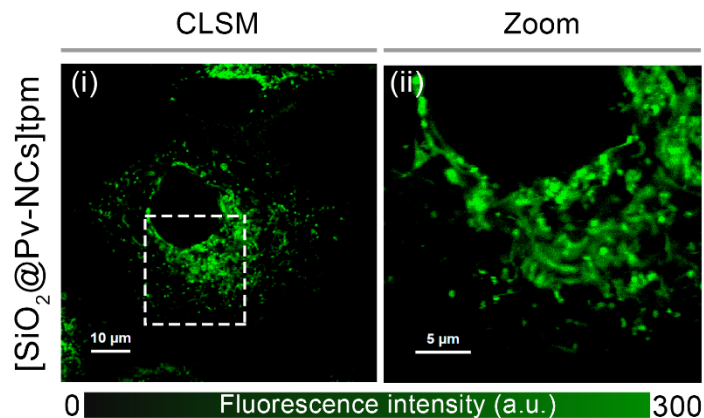


Fig. S17. Confocal laser scanning microscopy (CLSM) images of live HeLa cells treated with (i, ii) [SiO₂@Pv-NCs]tpm: (i) fluorescence image, and (ii) corresponding zoomed image of HeLa cell as indicated in the white dotted box in (i) depicting the tubular structure of mitochondria ($\lambda_{ex} = 470$ nm, $\lambda_{em} = 488 - 800$ nm, conc: 5×10^{-4} mg mL⁻¹); for (i) scale = 10 μ m, (ii) scale = 5 μ m. A common intensity scale is also presented for the fluorescence images.

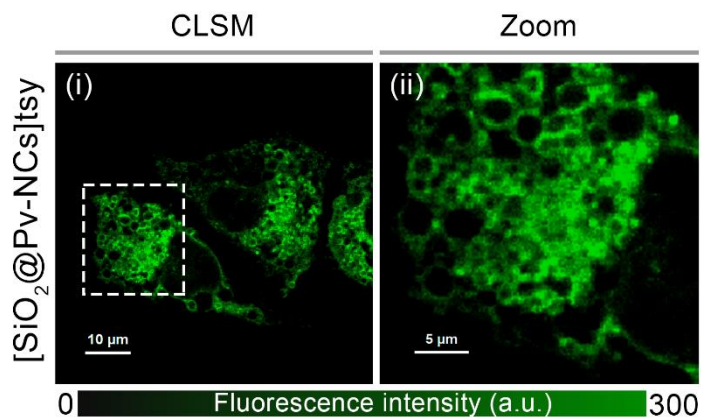


Fig. S18. CLSM images of live HeLa cells treated with (i, ii) [SiO₂@Pv-NCs]tsy: (i) fluorescence image and (ii) corresponding zoomed image of HeLa cell as indicated in the white dotted box in (i) depicting interconnected endoplasmic reticulum network structure ($\lambda_{ex} = 470$ nm, $\lambda_{em} = 488 - 800$ nm, conc: 5×10^{-4} mg mL⁻¹); for (i) scale = 10 μ m, (ii) scale = 5 μ m. A common intensity scale is also presented for the fluorescence images.

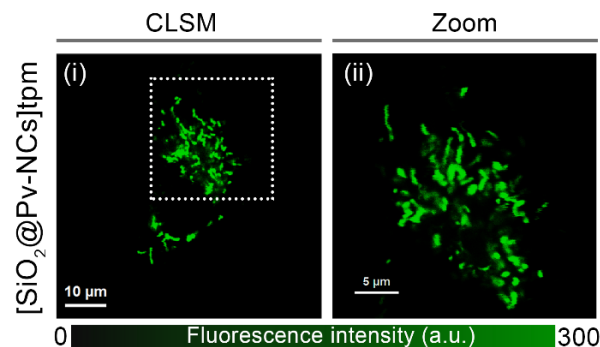


Fig. S19. CLSM images of fixed HeLa cells treated with (i-ii) $[\text{SiO}_2@\text{Pv-NCs}]_{\text{tpm}}$ ($\lambda_{\text{ex}} = 470 \text{ nm}$, $\lambda_{\text{em}} = 488 - 800 \text{ nm}$, conc: $5 \times 10^{-4} \text{ mg mL}^{-1}$). (i) CLSM image (scale = $10 \mu\text{m}$), and (ii) corresponding zoomed image of HeLa cells (scale = $5 \mu\text{m}$) as indicated in the white dotted box in (i) depicting the tubular structure of mitochondria. A common intensity scale is also presented for the fluorescence images.

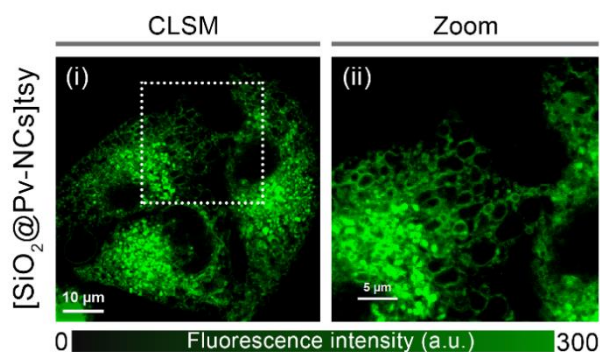


Fig. S20. CLSM images of fixed HeLa cells treated with (i-ii) $[\text{SiO}_2@\text{Pv-NCs}]_{\text{tsy}}$ ($\lambda_{\text{ex}} = 470 \text{ nm}$, $\lambda_{\text{em}} = 488 - 800 \text{ nm}$, conc: $5 \times 10^{-4} \text{ mg mL}^{-1}$). (i) CLSM image (scale = $10 \mu\text{m}$), and (ii) corresponding zoomed image of HeLa cells (scale = $5 \mu\text{m}$) as indicated in the white dotted box in (i) depicting interconnected endoplasmic reticulum network structure. A common intensity scale is also presented for the fluorescence images.

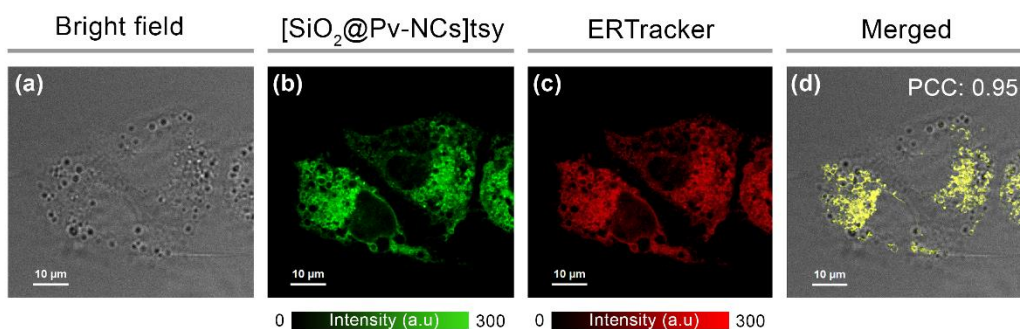


Fig. S21. Intracellular colocalization studies using CLSM of live HeLa cells; (a) bright field image, cells incubated with (b) $[\text{SiO}_2@\text{Pv-NCs}]_{\text{tsy}}$ ($\lambda_{\text{ex}} = 470 \text{ nm}$, $\lambda_{\text{em}} = 500 - 540 \text{ nm}$, conc: $5 \times 10^{-4} \text{ mg mL}^{-1}$), (c) ERTrackerTM Red ($\lambda_{\text{ex}} = 640 \text{ nm}$, $\lambda_{\text{em}} = 650 - 690 \text{ nm}$, $0.5 \mu\text{M}$), (d) merged image of (a), (b), and (c) indicates ER-targeting ability of $[\text{SiO}_2@\text{Pv-NCs}]_{\text{tsy}}$ (Pearson's colocalization coefficient, PCC: 0.95); scale = $10 \mu\text{m}$. Common intensity scales are also provided for the fluorescence images.

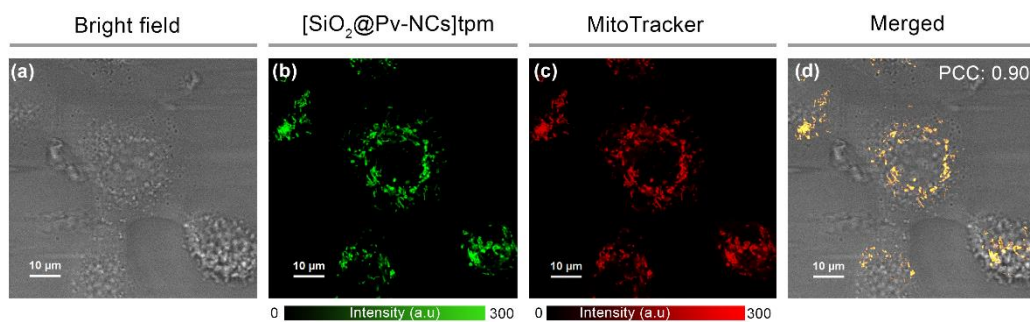


Fig. S22. Intracellular colocalization studies using CLSM of live HeLa cells; (a) bright field image, cells incubated with (b) $[\text{SiO}_2@\text{Pv-NCs}]_{\text{tpm}}$ ($\lambda_{\text{ex}} = 470 \text{ nm}$, $\lambda_{\text{em}} = 500 - 540 \text{ nm}$, conc: $5 \times 10^{-4} \text{ mg mL}^{-1}$), (c) MitoTrackerTM Deep Red ($\lambda_{\text{ex}} = 640 \text{ nm}$, $\lambda_{\text{em}} = 650 - 690 \text{ nm}$, $0.5 \mu\text{M}$), (d) merged image of (a), (b), and (c) indicates mitochondria-targeting ability of $[\text{SiO}_2@\text{Pv-NCs}]_{\text{tpm}}$ (Pearson's colocalization coefficient, PCC: 0.95); scale = $10 \mu\text{m}$. Common intensity scales are also provided for the fluorescence images.

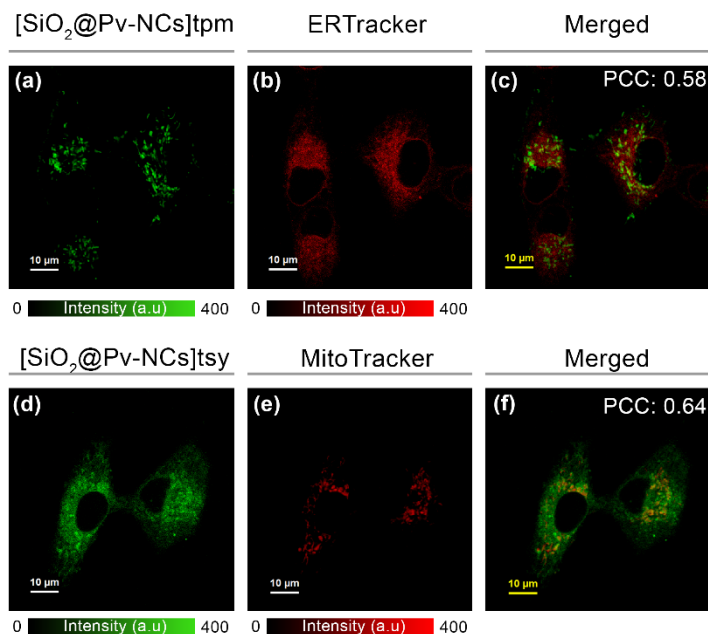


Fig. S23. CLSM images of HeLa cells co-incubated with (a) $[\text{SiO}_2@\text{Pv-NCs}]_{\text{tpm}}$ ($\lambda_{\text{ex}} = 470 \text{ nm}$, $\lambda_{\text{em}} = 500 - 540 \text{ nm}$), (b) commercial endoplasmic reticulum (ER)-targeting dye, ERTrackerTM Red ($\lambda_{\text{ex}} = 640 \text{ nm}$, $\lambda_{\text{em}} = 650 - 690 \text{ nm}$), and (c) merged image of (a) and (b) showing low Pearson's coefficient of colocalization (PCC) of 0.58, indicating no specific staining of ER by $[\text{SiO}_2@\text{Pv-NCs}]_{\text{tpm}}$. Confocal laser scanning microscopy (CLSM) images of HeLa cells co-incubated with (d) $[\text{SiO}_2@\text{Pv-NCs}]_{\text{tsy}}$ ($\lambda_{\text{ex}} = 470 \text{ nm}$, $\lambda_{\text{em}} = 500 - 540 \text{ nm}$), (e) commercial mitochondria-targeting dye, MitoTrackerTM Deep Red ($\lambda_{\text{ex}} = 640 \text{ nm}$, $\lambda_{\text{em}} = 650 - 690 \text{ nm}$), and (f) merged image of (d) and (e) showing low PCC value of 0.64, indicating no specific staining of mitochondria by $[\text{SiO}_2@\text{Pv-NCs}]_{\text{tsy}}$; scale = $10 \mu\text{m}$. A common intensity scale is presented for the fluorescence images.

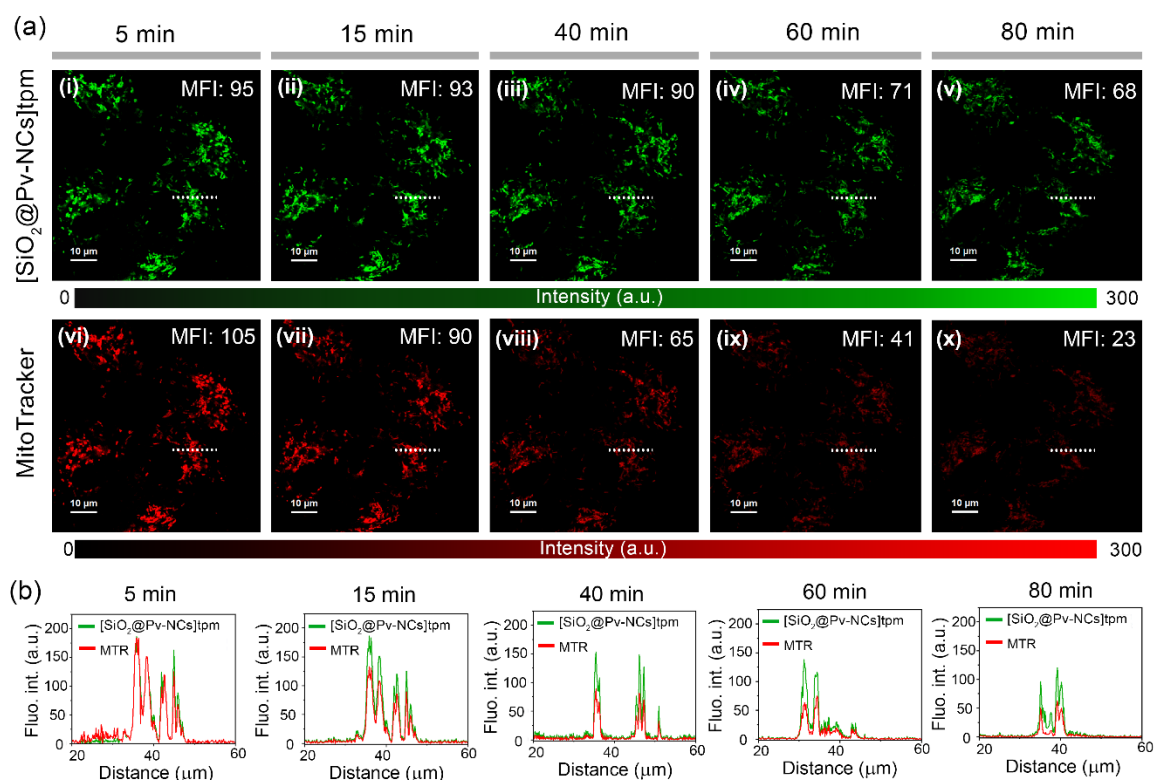


Fig. S24. (a) CLSM images of live HeLa cells co-incubated with [SiO₂@Pv-NCs]tpm and commercial mitochondria targeting dye, MitoTrackerTM Deep Red (MTR) depicting higher photostability of [SiO₂@Pv-NCs]tpm over a time span of 80 mins under continuous laser irradiation of constant power (laser power = 0.3 μW, power density = 1.52 W mm⁻²). Images of HeLa cells co-incubated with (i - v) [SiO₂@Pv-NCs]tpm ($\lambda_{\text{ex}} = 470 \text{ nm}$, $\lambda_{\text{em}} = 500 - 540 \text{ nm}$), and (vi - x) MTR ($\lambda_{\text{ex}} = 640 \text{ nm}$, $\lambda_{\text{em}} = 650 - 690 \text{ nm}$); a common intensity scale is presented for the fluorescence images; scale bar = 10 μm. Corresponding mean fluorescence intensities (MFIs) for the respective images are also indicated. (b) Corresponding intracellular fluorescence intensity profiles of [SiO₂@Pv-NCs]tpm and MTR along the white dotted lines depicted in (a).

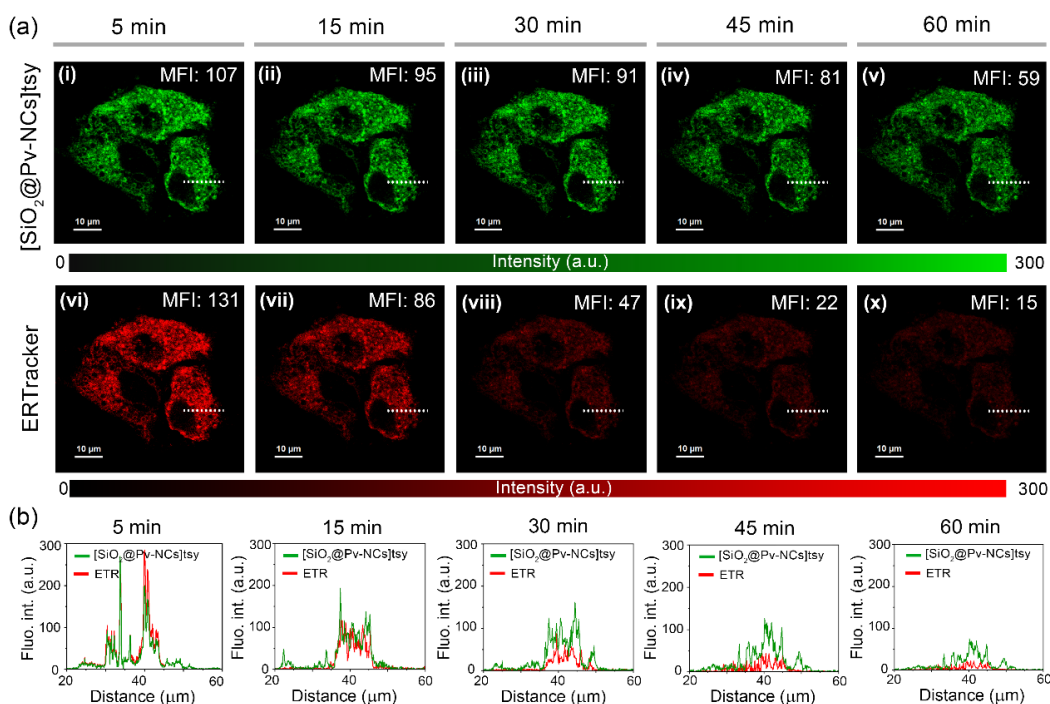


Fig. S25. (a) CLSM images of live HeLa cells co-incubated with $[\text{SiO}_2@\text{Pv-NCs}]\text{tsy}$ and commercial endoplasmic reticulum targeting dye, ERTrackerTM Red (ETR) depicting higher photostability of $[\text{SiO}_2@\text{Pv-NCs}]\text{tsy}$ over a time span of 60 mins under continuous laser irradiation of constant power (laser power = $0.3 \mu\text{W}$, power density = 1.52 W mm^{-2}). Images of HeLa cells co-incubated with (i - v) $[\text{SiO}_2@\text{Pv-NCs}]\text{tsy}$ ($\lambda_{\text{ex}} = 470 \text{ nm}$, $\lambda_{\text{em}} = 500 - 540 \text{ nm}$), and (vi - x) ETR ($\lambda_{\text{ex}} = 640 \text{ nm}$, $\lambda_{\text{em}} = 650 - 690 \text{ nm}$); a common intensity scale is presented for the fluorescence images; scale bar = $10 \mu\text{m}$. Corresponding mean fluorescence intensities (MFIs) for the respective images are also indicated. (b) Corresponding intracellular fluorescence intensity profiles of $[\text{SiO}_2@\text{Pv-NCs}]\text{tsy}$ and ETR along the white dotted lines depicted in (a).

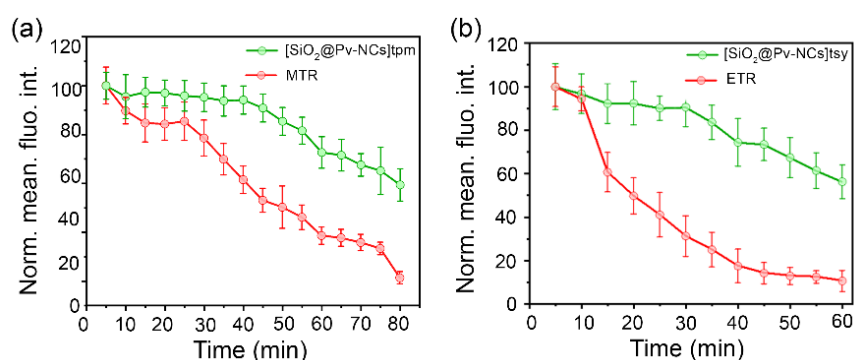


Fig. S26. Intracellular photostability of (a) $[\text{SiO}_2@\text{Pv-NCs}]\text{tpm}$ ($\lambda_{\text{ex}} = 470 \text{ nm}$, $\lambda_{\text{em}} = 500 - 540 \text{ nm}$) and MTR ($\lambda_{\text{ex}} = 640 \text{ nm}$, $\lambda_{\text{em}} = 650 - 690 \text{ nm}$), and (b) $[\text{SiO}_2@\text{Pv-NCs}]\text{tsy}$ ($\lambda_{\text{ex}} = 470 \text{ nm}$, $\lambda_{\text{em}} = 500 - 540 \text{ nm}$) and ETR ($\lambda_{\text{ex}} = 640 \text{ nm}$, $\lambda_{\text{em}} = 650 - 690 \text{ nm}$); normalized mean fluorescence intensity variation of the probe stained HeLa cells for continuous laser irradiation of (a) 80 min and (b) 60 min (laser power = $0.3 \mu\text{W}$, power density = 1.52 W mm^{-2}) showing superior photostability of $[\text{SiO}_2@\text{Pv-NCs}]\text{tpm}$ and $[\text{SiO}_2@\text{Pv-NCs}]\text{tsy}$. The error bar is plotted as mean \pm standard deviation ($n = 3$).

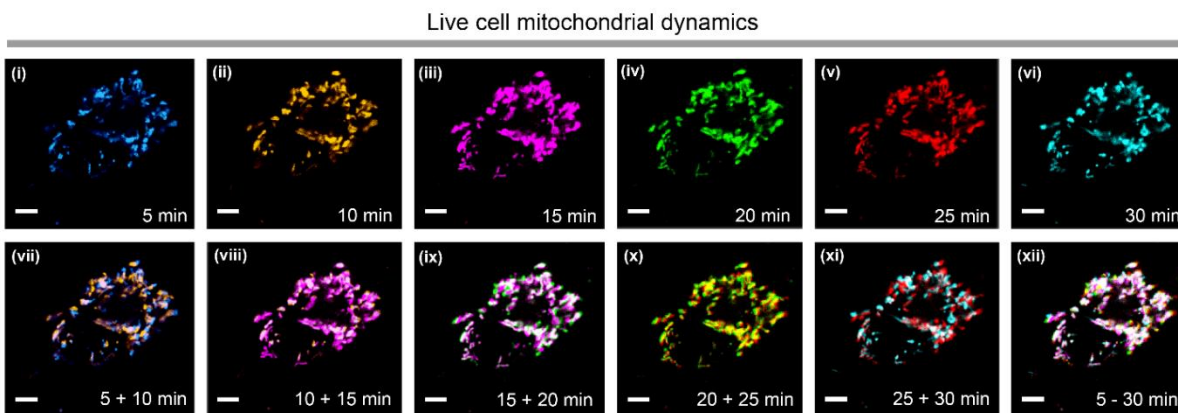


Fig. S27. Pseudocolor-CLSM images revealing mitochondrial dynamics in live HeLa cells stained with $[\text{SiO}_2@\text{Pv-NCs}]\text{tpm}$ ($\lambda_{\text{ex}} = 470 \text{ nm}$, $\lambda_{\text{em}} = 488 - 800 \text{ nm}$) at different time intervals: (i) 5, (ii) 10, (iii) 15, (iv) 20, (v) 25, and (v) 30 mins. The merged images of (vii) i and ii, (viii) ii and iii, (ix) iii and iv, (x) iv and v, (xi) v and vi, and (xii) i to v depict the dynamic nature of mitochondria in live cells; scale = $4 \mu\text{m}$.

The nanocrystals showed multi-day imaging ability in HeLa cells. HeLa cells were incubated with nanocrystals for 30 mins in DMEM under humid conditions. After the incubation the cells were washed with PBS thrice, fresh DMEM was added to the cells and the cells were incubated for respective days (1, 2, and 3 days). On the respective day of imaging, the cells were washed with PBS, and FluoroBrite™ DMEM was added to the cells before imaging. The results suggest that the nanocrystals incubated cells could be imaged for up to 3 days.

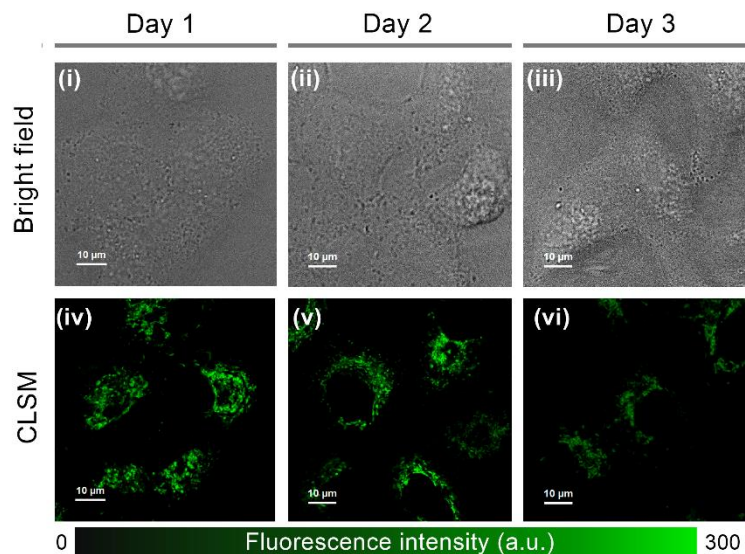


Fig. S28. Long-term imaging of HeLa cells employing $[\text{SiO}_2@\text{Pv-NCs}]\text{tpm}$ after single-time incubation (30 min) for three days; (i - iii) bright field images, (iv -vi) fluorescence images ($\lambda_{\text{ex}} = 470 \text{ nm}$, $\lambda_{\text{em}} = 488 - 800 \text{ nm}$); a common intensity scale is also presented for the fluorescence images; scale = $10 \mu\text{m}$.

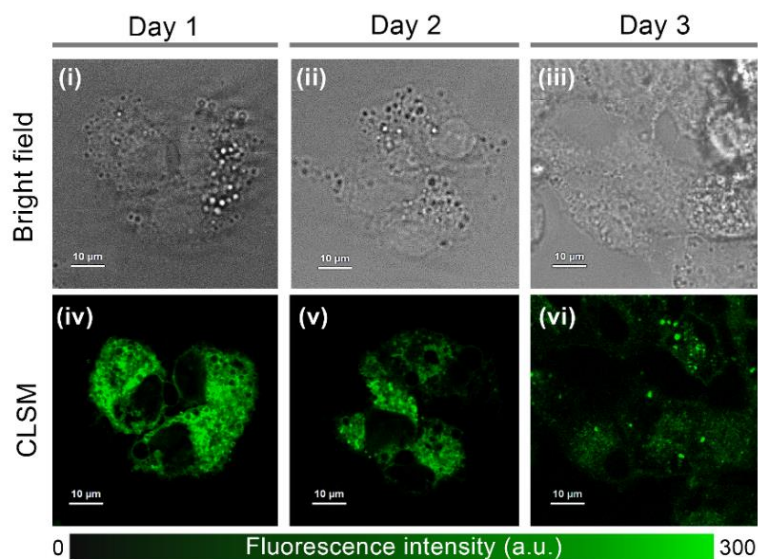


Fig. S29. Long-term imaging of HeLa cells employing $[\text{SiO}_2@\text{Pv-NCs}]_{\text{tsy}}$ after single-time incubation (30 min) for three days; (i - iii) bright field images, (iv -vi) fluorescence images ($\lambda_{\text{ex}} = 470 \text{ nm}$, $\lambda_{\text{em}} = 488 - 800 \text{ nm}$); a common intensity scale is also presented for the fluorescence images; scale = $10 \mu\text{m}$.

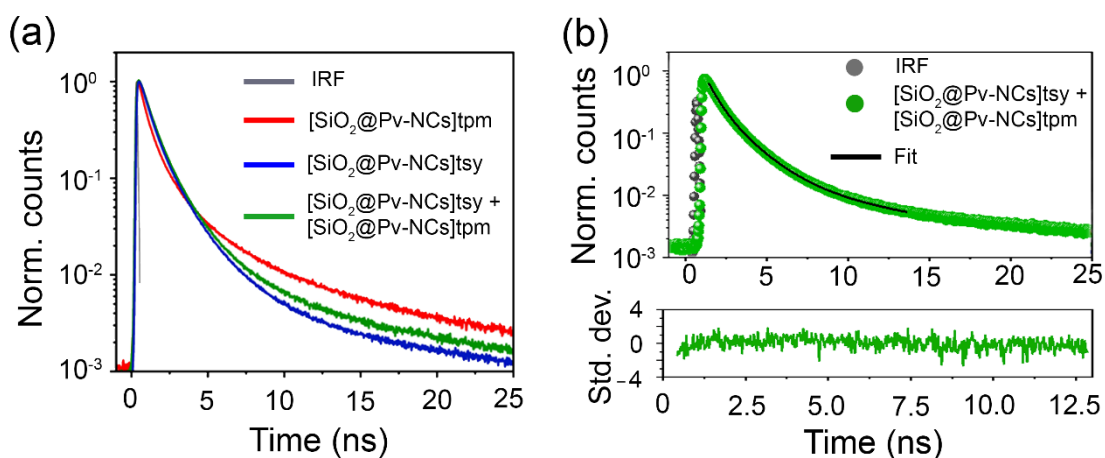


Fig. S30. (a) Intracellular decay profiles of $[\text{SiO}_2@\text{Pv-NCs}]_{\text{tpm}}$ (red), $[\text{SiO}_2@\text{Pv-NCs}]_{\text{tsy}}$ (blue), and co-incubated $[\text{SiO}_2@\text{Pv-NCs}]_{\text{tpm}}$ and $[\text{SiO}_2@\text{Pv-NCs}]_{\text{tsy}}$ (green) in HeLa cells. (b) Intracellular decay profile of co-incubated $[\text{SiO}_2@\text{Pv-NCs}]_{\text{tpm}}$ and $[\text{SiO}_2@\text{Pv-NCs}]_{\text{tsy}}$ (green) in HeLa cells, corresponding fit, and residual ($\chi^2 = 1.15$) as obtained from the pattern matching analysis.

References

1. Y. Wang, X. Li, V. Nalla, H. Zeng and H. Sun, *Adv. Funct. Mater.*, 2017, **27**, 1605088.
2. S. Li, D. Lei, W. Ren, X. Guo, S. Wu, Y. Zhu, A. L. Rogach, M. Chhowalla and A. K. Y. Jen, *Nat. Commun.*, 2020, **11**, 1192.
3. R. Tiwari, P. S. Shinde, S. Sreedharan, A. K. Dey, K. A. Vallis, S. B. Mhaske, S. K. Pramanik and A. Das, *Chem. Sci.*, 2021, **12**, 2667-2673.
4. N. Fiuza-Maneiro, K. Sun, I. López-Fernández, S. Gómez-Graña, P. Müller-Buschbaum and L. Polavarapu, *ACS Energy Lett.*, 2023, **8**, 1152-1191.
5. S. Kundu, A. Chowdhury, S. Nandi, K. Bhattacharyya and A. Patra, *Chem. Sci.*, 2021, **12**, 5874-5882.
6. (a) R. Thavarajah, V. K. Mudimbaimannar, J. Elizabeth, U. K. Rao and K. Ranganathan, *J. Oral Maxillofac. Pathol.*, 2012, **16**, 400. (b) C. Liu, D.L. Steer, H. Song and L. He, *J. Phys. Chem. Lett.*, 2022, **13**, 1609-1616.
7. (a) A. J. Hobro and N. I. Smith, *Vibra. Spec.*, 2017, **91**, 31–45; (b) J. St-Laurent, M. Boulay, P. Prince, E. Bissonnette, L. Boulet; *J. Immunol. Methods.*, 2006, **308**, 36-42; (c) Y. Qin, W. Jiang, A. Li, M. Gao, H. Liu, Y. Gao, X. Tian and G. Gong, *Biomol.*, 2021, **11**, 711.
8. (a) J. C. Thiele, D. A. Helmerich, N. Oleksiievets, R. Tsukanov, E. Butkevich, M. Sauer, O. Nevskiy and J. Enderlein, *ACS Nano*, 2020, **14**, 14190-14200. (b) J. C. Thiele, O. Nevskiy, D. A. Helmerich, M. Sauer and J. Enderlein, *Front. Bioinform.*, 2021, **1**, 740281.
9. M. S. Frei, B. Koch, J. Hiblot and K. Johnsson, *ACS Chem. Biol.*, 2022, **17**, 1321-1327.